Engineering Science and Technology, an International Journal 44 (2023) 101469

HOSTED BY

Contents lists available at ScienceDirect

Engineering Science and Technology, an International Journal

journal homepage: www.elsevier.com/locate/jestch

Full Length Article

Energy efficiency model-based Digital shadow for Induction motors: Towards the implementation of a Digital Twin

Adamou Amadou Adamou *, Chakib Alaoui

Euromed University of Fez, BP 51, Route Nationale de Meknès (Rondpoint Ben Souda), 30070 Fès, Morocco

ARTICLE INFO

Article history:
Received 14 November 2022
Revised 4 May 2023
Accepted 15 June 2023
Available online 24 June 2023

Keywords:
Induction motors
Energy efficiency
Digital shadow
Digital twin
ANFIS

ABSTRACT

The 4th industrial revolution requires the tracking and optimization of energy consumption using an intelligent energy management system (IEMS). Such a system needs accurate real-time energy information to operate industrial machines, where Induction Motors (IMs) represent 42.2% of the global energy consumption. This paper addresses the problems of data acquisition for Induction motors in the context of Industry 4.0 (I4.0) where precision, real-time constraints, and optimal operations play a major role in decision-making. A new vision of Digital Shadow (DS) is proposed for the energy efficiency (EE) of IMs. A hybrid model consisting of a data-driven model and a physics-based model is developed to represent the machine efficiency information in real-time (RT). The proposed method is developed based on a two-stage procedure. Firstly, the IM EE model is established by considering Stator joule losses, core losses, rotor joule losses, friction, and windage losses, in addition to the stray losses to create an improved model. This was established based on the double cage model where core loss resistance is added. Secondly, the machine's losses and efficiency are visualized using the 8 electrical circuit parameters (ECP) from the double cage model in addition to the rated speed and test temperature. The parameters estimation in RT incurred complexities and required the use of Adaptive Neuro-Fuzzy Inference System (ANFIS)-based modeling. The proposed model was developed using Fuzzy Logic Toolbox and Neuro-Fuzzy Designer app from MATLAB by training Sugeno systems. 8 ANFIS MATLAB models are trained to estimate each of the 8 ECP from the double cage model by using standard inputs. The training and testing dataset is constituted by the experimental data of the ECPs were calculated using the FSOLVE function to solve the nonlinear system formed by 60 motors from 8 manufacturers' data such as voltage, number of pole-pairs, rated output power, rated torque, current, starting current, maximum torque and the power factor. Finally, the proposed method is validated experimentally using a 1.5 KW, 400/230 V, 50 Hz squirrel cage induction motor (SCIM) for linear speed control. The EE, Torque, and losses are visualized through the proposed model using MATLAB/SIMULINK. The mean value of the RMSE for the eight estimated ECPs are 7.57e-05, and 5.73e-01 respectively for training and testing while the mean values of the MAE are 2.06e-05, and 3.79e-01 respectively for training and testing. The errors of the EE estimation w.r.t the measured EE at rated condition, are RMSE = 0.205, and MAE = 0.1671. These results show that the proposed model can be implemented in the industry to monitor the machine EE and its losses.

1. Introduction

The development of industrial technologies imposes a new vision that is I4.0 where machines are connected through IoT technologies, thereby allowing managers to take decisions rapidly. The complexity of industrial architectures in data acquisition necessitates more advanced sensors and more sophisticated computer networks. In this trend, Cyber-Physical Systems (CPS) are used for managing interconnected systems between their physical assets and computational capabilities [1]. Manufacturing systems can monitor their self-improving physical assets using digital twin (DT) or cyber twin, where a smart reactive decision is possible through real-time (RT) communication, and the feedback collected by AI algorithm [2]. All the mentioned technologies required energy to operate, data computing, transmission, monitoring, and control. Thereby, scientific literature, research projects, and industry expertise make it clear that there is a need for a novel and robust platform capable of providing more energy information

* Corresponding author.
E-mail addresses: a.amadou@ueuromed.org (A. Amadou Adamou), c.alaoui@insa.ueuromed.org (C. Alaoui).

https://doi.org/10.1016/j.jestch.2023.101469
2215-0986/

Nomenclature

η	Efficiency
P	Rated mechanical power
Q	Reactive power
V_S	Stator voltage in Y configuration
p	Number of pairs of poles
T_{FL}	Full-load torque
T_M	Maximum torque
T_{ST}	Starting torque
P_{sj}	Stator joule loss
P_c	Core losses
P_{rj}	Rotor joule loss
P_m	Mechanical losses
P_{stray}	Stray losses
R_{ho}	Winding resistance, in ohms, corrected to the temperature T_{ho},
R_{co}	Known value of the winding resistance, in ohms, at the temperature T_{co},
T_{ho}	Temperature of the winding resistance in °C when R_{ho} was measured at the hot test,
T_{co}	Temperature of the winding resistance in °C when R_{co} was measured at the cold test,
k_1	234.5 for 100% IACS conductivity copper, or 225 for aluminum, based on a volume conductivity of 62%,
$T(t)$	Temperature of the winding resistance in °C at time t,
Δt	Time between the cold and the hot test,
R_S	Stator resistance per phase
R_C	Core resistance per phase
R_1	Inner-cage rotor resistance
R_2	Outer-cage rotor resistance
X_S, L_S	Stator leakage reactance and inductance per phase
X_m, L_m	Magnetizing reactance and inductance per phase
X_1, L_1	Inner-cage rotor reactance and inductance per phase
X_2, L_2	Outer-cage rotor reactance and inductance per phase
s	Slip
SCIM	Squirrel Cage Induction Motor
BR, LR	Blocked or locked rotor test
*I*4.0	Industry 4.0

monitoring, integration, repository, and analytics towards future energy-efficient manufacturing [3 4 5]. A large volume of data from various industries and locations is required to establish a better Energy Management System (EMS). Furthermore, due to the heterogeneity of the data, not all actors within the industrial ecosystem can efficiently exploit the data [6].

To face these challenges, a DT is used to digitalize the system and monitor the energy information in RT coming from the physical assets through a dynamic model. The development of the energy efficiency model-based DT in the I4.0 context passes through the DS which consists in collecting real-time heterogeneous energy data to be exploited in the model, hence improving the simulation of energy consumption for all the ecosystem of loads [7]. Nevertheless, the heterogeneity of energy data types and the lack of communication between entities are blocking the implementation of energy-based DT and DS in a real industry. Hence, to standardize data collection, the energy efficiency of each entity is used starting with a single machine.

Achieving high energy efficiency with low cost remains a challenge up to this day. Novel EMS architectures allow to control and improve the efficiency of industrial systems without affecting their operational performance. According to the International Energy Agency (IEA) [8], 53% of electrical energy consumption goes to Electric Drives (ED) or Electric Motor-Driven Systems (EMDS). Among the EMDS, 77% of the electrical energy consumption is due to medium-sized motors, whereas 80% are Induction Motors of different types [9]. The use of a large quantity of IMs makes them a good candidate for energy efficiency improvements. The medium-sized IMs with 84% energy efficiency consume 10,500TWh per year, so if a mere one percent of EE is improved during the operation, 105 TWh[1] could be saved [10]. The efficiency of IMs has emerged as having the biggest potential for energy saving [11]. In these trends, collecting significant energy information on IMs is crucial. Hence, Improving the efficiency of IMs cannot be achieved without an accurate estimation of all losses of said motors, in particular, the stray losses (SL). Beyond the design stage, optimal operation of IM requires an accurate RT determination of efficiency, hence stray load losses.

[1] According to [10] 10,500 TWh is the total annual energy consumption of mid-sized MIs. Indeed, when we improve their efficiency by 1% during their operation, we could save about 105TW per year.

The EE is a comprehensive indicator of both the energy consumption and the state of health of the machine. A potential practical application of this approach is to develop an EE-based predictive maintenance method, which utilizes historical data of machine EE [12]. To meet the I4.0 goals, an energy management system can be developed using all the IMs energy information, starting at a small level with one motor to a bigger scale where all the IMs energy information is collected and processed for control based on the industry energy goal. This paper proposes to include the core loss, friction and windage losses, and stray loss in the double cage model into the DT to improve its accuracy in real-time and In-situ environments. To the best of our knowledge, this was never done before, hence the improvements obtained in the experimental validation. In this paper, an energy efficiency-based DS for SCIM is developed. This consists of the development of an IM energy efficiency model which is operated by the measured magnitudes such as Voltage, Current, power factor, internal temperature, and the operational speed by considering the in-situ aspect. In this paper, a DS is established by developing a dynamic model of the IM using the following procedures. Firstly, the proposed double cage model, which consists of 8 Electrical Equivalent Circuit Parameters (ECPs) is validated using a 132 kW, 380/660 V 50 Hz SCIM. Then, 8 ECPs of IM are found by a numerical method using 8 manufacturer data of 60 motors with different rated power. Then, to predict each ECPs for implementation, 8 ANFIS MATLAB models are trained and tested using the experimental dataset established by the previous numerical method where the outputs are the ECPs and the input are the 8 manufacturers' data such as, pole-pairs, rated output power, per unit maximum and rated torque, per unit starting current, the rms of the input voltage, current and the power factor. Finally, a 1.5 KW, 400/230 V, 50 Hz SCIM is used to validate the proposed method using the MATLAB/SIMULINK environment by comparing the measured EE w.r.t the calculated EE from the proposed method. The changes of the input magnitudes in the model during the operation of the machine represent the RT EE, hence the DS is built from this. As the model is also rotor speed-dependent, a tachometer based on the stroboscopic technique is a solution to measure the rotor speed in RT in situ.

The utilization of the ANFIS algorithm in real-time applications addressing issues related to induction motors (IMs) is primarily focused on control, estimation, and prediction. A review of an

Table 1
Overview of In-Situ EE Estimation Methods.

REFERENCES	METHODS USED	STUDY LIMITATION
[27]	Survey Of Methods for in-Service IM Energy efficiency estimation. Air Gap Torque (AGT) method is judged the best)A perspective of improvement has been proposedThe general approach to developing nonintrusive methods is proposed	The selected methods are difficult to be used in situ without improvement (the accuracy of these methods is high when the load is above 50%)
[28]	Segregated method (expressed the losses based on Sankey diagram and T model)Helwig's methods to eliminate the correlations of the coefficientsThe minimum chi-square method	Accuracy of loss estimation is not the main goalThe excess Eddy Current is ignoredThe insulation losses are neglectedAll the rotor losses are neglectedEliminate the non-linearity to identify the model
[29]	Develop an accurate model of Eddy Current and Hysteresis taking into account the temperature dependency of both lossDevelop a global model of core loss	The skin effect is not taken into accountThe excess core loss is ignored in the core loss expression
[30]	Vibration Tests with an Accelerometer + Nameplate data	Need other measurements for improvement such as: Rated speed correction, Temperature compensation, and Voltage compensation
[31]	In-situ Efficiency estimation based on the positive and negative sequence single cage equivalent circuit for unbalanced supply conditions. Nonintrusive speed estimation technique based on the machine-current-signature analysis.	The 3 main sources ([10]) of the stray loss are not taken into consideration The mechanical loss is not consideredThe machine transient state is not considered in their algorithm
[32]	In-situ Efficiency estimation based on ECPs estimated by the combination of the genetic algorithm and the IEEE Form F2-Method F1.The speed was estimated using the notch filter algorithm.	The main sources of the stray loss are not taken into consideration

ANFIS-based IM controller is presented in [13]. Furthermore, in [14], the authors describe the development of an ANFIS torque controller method, which is implemented in an induction motor drive through decoupling feedback linearization. The aim is to enhance both dynamic and steady-state performance. However, there have been efforts to apply the ANFIS algorithm for estimating the ECPs of IMs. For instance, in [15], two novel methods based on artificial neural networks (ANN) and ANFIS are proposed for predicting the induction motor parameters in the single-cage and double-cage models. In [16], the performance of ANFIS is compared to the feed-forward neural network (FFNN) and Elman neural network (ENN) for estimating the ECPs of the SCIM. Hence, in this study, the ANFIS algorithm is used for the RT estimation of the ECPs.

This paper is organized as follows. In section 2, the research significance and novelty of the work are highlighted. In section 3, a literature review is carried out on induction motor DT implementation in I4.0, where the concept of DT and DS have been introduced, and the role of the dynamic model in DT development is discussed. In section 4, the development of the EE model for the DS application of induction motors is highlighted. In section 5, simulation results are exposed where the development of the optimum ANFIS model is highlighted, and the energy efficiency is monitored using MATLAB/SIMULINK. In sections 6 and 7, a brief conclusion and a perspective idea for future works are proposed.

2. Research significance and novelty of work

The induction motor is typically represented by its electrical equivalent circuit, and the parameters of this circuit are either extracted or estimated depending on the specific model being used. In the case of the Simple Cage model, the parameters are extracted through routine tests, including the No-load test, Blocked Rotor test, and DC test. However, the Double Cage model requires estimation of its parameters due to their large number. Estimating the ECPs for the Double Cage model has been the subject of extensive research, with the classical estimation method relying on manufacturer data obtained through routine tests. This nonlinear system is usually solved using a numerical method based on a least-squares algorithm, such as the Gauss-Newton or Levenberg-Marquardt methods [17]–[19]. Additionally, artificial intelligence-based algorithms (AIA) have also been employed to estimate ECPs for IMs [15,16,20]. Due to their ease of implementation and computational efficiency, AIA algorithms can be used for RT applications of ECPs estimation for induction motors.

The research activities dealing with the DT application for IMs focuses on the design, predictive maintenance, and control aspects of the machine. To the best of our knowledge, no published research can be found about IMs DT implementation based on the I4.0 reference architecture model. In [21], the five-dimension DT model is defined as a reference and global architecture for a big and large-scale DT implementation but no study is conducted for IM DT implementation based on this model [22]–[24]. In [25], a slip ring induction motor digital model is developed using a pre-computed finite element model, and then the DS was integrated for a RT computation of electromagnetic quantities of the motor. In [26], an analytical model of IM is improved by adding in the conventional segregated method, the skin effect, the loading, and the field-weakening operation. Thereby the result of the mentioned work shows that the improved analytical model is more accurate than the FEM and it can be used for IM DT development. In [23] the concept of the next-generation DT is redefined and the DT application for electrical machine predictive maintenance methods is reviewed. According to the literature, no study develops a DS for IM based on energy efficiency, where the Induction motor Energy efficiency model based on the DT application is highlighted by computing in RT the losses and energy efficiency model and taking into consideration the in-situ aspect.[2] There are many methods for EE estimation in-situ but all these methods don't meet the I4.0 needs. Among the existing method, some are summarized in Table 1.

3. IMs energy efficiency model-based DT implementation in I4.0

The EMS required energy consumption data for its AI algorithms to optimize industrial energy consumption. It is not evident to collect relevant energy data in the industry while considering the in-situ aspect where some parts of the machines may not be accessible. The alternative is to build an energy efficiency model of the machine, which can operate with only the easily accessible parameters, such as current, voltage, and temperature. Such a model uses fewer sensor data due to its AI-based algorithms, which estimate the losses and, thus, the EE of the machine. The first step to estimate the EE of the machine in real-time is accomplished through its DS. However, further steps are needed for the full deployment of its DT, as illustrated in Fig. 1 [33].

[2] Take into consideration the industrial constraint where the interested machines are installed.

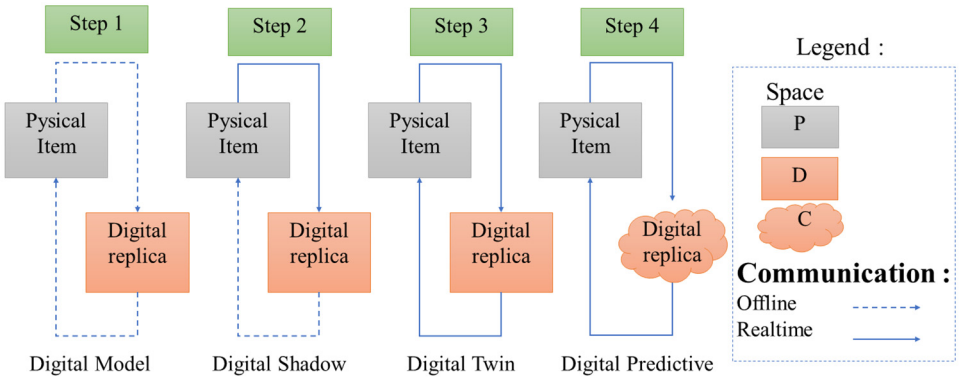

Fig. 1. DT Integration Levels in the Reference Architecture Model proposed in [33].

A DT is a concept of the modern industry that first appeared in 2002 at the University of Michigan during a presentation for the formation of a Product Lifecycle Management (PLM) center. NASA's Apollo space program was the first to use the DT concept where they highlighted 2 vehicles, one on Earth that can mirror, simulate, and predict the conditions of another vehicle in space [34]. Hribernik et al. [35] introduced the concept of "product avatar" which is similar to the "DT". In the I4.0 context, the digital object regulates and improves the condition of the physical item. The German Electrical and Electronic Manufacturers' Association developed the Reference Architecture Model for I4.0 (RAMI 4.0) to support the new industrial revolution initiatives based on a holistic approach of manufacturing companies. RAMI 4.0 provides companies with a holistic framework to develop future products and business models using a three-dimensional map (such as layers, life cycle, and hierarchy level or data flow) in a structured manner, complemented by pillars of the new industrial era [36]. The proposed RAMI, shown in Fig. 2, is for a single machine. However, when validated, this system can be duplicated for several machines that may be installed in an industrial facility. To develop a large-scale DT for IMs, the 5-dimension DT can be considered as described in [22].

3.1. The role of DS in the development of the DT for IM

Real-time monitoring of the machine's EE through a dynamic model is an EE-based DS, which reflects the machine's energy behavior and provides insight into the machine's health [37]. Even though these terms are frequently used interchangeably, it is essential to understand that "digital model", "DS", and "DT" refer to distinct concepts. The DS plays a vital role in enhancing the user interface by providing a digital image of machines and assembly stations using real-time data in industries that use ICT [7]. Moreover, a separate DS may be used for each machine in an industrial environment where a large number of machines are needed. This solution may reduce the difficulties associated with the heterogeneity of data and the lack of communication between departments as they frequently occur in an industrial environment [6]. Since the DS represents a physical model with a one-way data flow, all the information that the operator receives through the HMI depends on the DS model [38]. Therefore, achieving the development of DS is crucial for DT implementation.

3.2. The role of dynamics and evolutionary model in IM DT development

The development of a DT imposes the use of a model in all the processes as shown in Fig. 2, generally, it starts with a so-called nominal model [39]. The latter is the digital initial model which

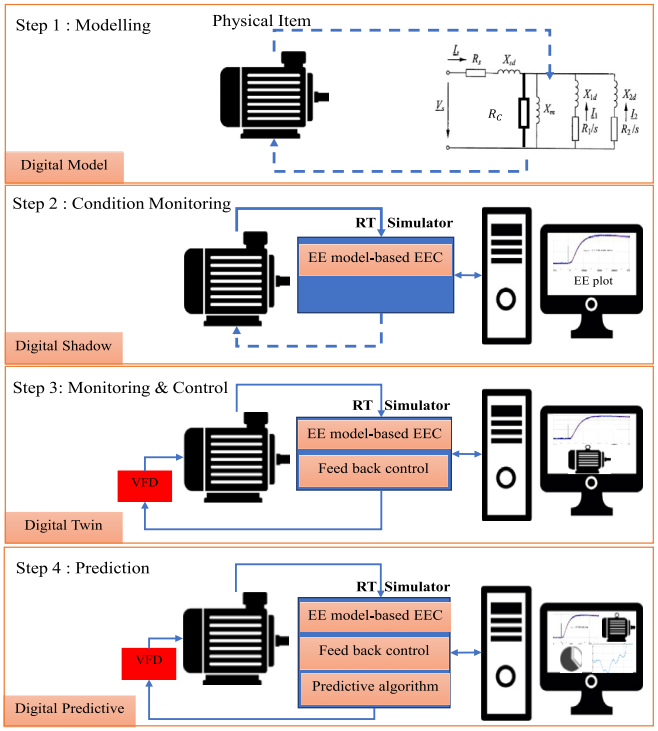

Fig. 2. Proposed reference Architecture model for IM DT implementation.

is a physic-based model that implements, validates, and identifies w.r.t the studied system. Beyond the objective of the DT and the change in the industry, only a dynamic model can represent the behavior of the machine in RT. It's also important to have a model where the computation time is less than the time between two updates of the inputs magnitudes, otherwise, the system will accumulate the error and lose its dynamic, hence, a RT simulator help achieve this objective. IM model must have a temperature, voltage, and current dependency and must take into consideration the varying of these magnitudes. The DT updates itself by tracking the physical system and also by adjusting some parameters to improve the physical twin. So, an evolutionary model is needed to achieve this objective. The evolutionary model uses real-time AI optimization tools such as machine learning and reinforcement learning.

4. IM EE-based DS: Digital model expression

This part aims to find an accurate and dynamic analytical model that can mirror the real-time energy consumption of IM based on

its electrical equivalent circuit. Among the existing models, the double cage model is used in this study to perform the fidelity of the model. The proposed model estimates the Energy Efficiency using Stator copper losses, Stator and rotor core losses, rotor cage losses, mechanical losses (windage and friction), and stray loss. According to the works done by J.Pedra et al. [18], the double-cage model (Fig. 3 (a)) must be used to obtain realistic behavior of the IM. Additionally, the accuracy of the double cage model can be increased further by adding core loss resistance (Fig. 3 (b)).

4.1. Using IM double cage model with core loss resistance

To improve the precision of the double cage model, the core loss has been incorporated. To evaluate the effectiveness of this addition, a comparison has been made between two versions of the double cage model, as shown in Fig. 3 (a) and (b), w.r.t the experimental data obtained from the manufacturer datasheet of a 132 kW, 380/660 V 50 Hz motor, as presented in Table 2. The ECPs listed in Table 3 have been determined using the algorithm proposed in [19]. Simulation results for the torque-slip and current-slip curves demonstrate that the inclusion of core loss resistance significantly improves the accuracy of the model, as depicted in Fig. 4.

$$\Gamma(s) = \frac{3p}{\omega_s}\left([I_1(s)]^2\frac{R_1}{s} + [I_2(s)]^2\frac{R_2}{s}\right); I_s(s) = \frac{V_s}{R_s + jX_{sd} + Z_p} \quad (1)$$

Where $I_1(s) = -\frac{Z_s(s)\,.\,I_s(s)}{R_1/s + jX_{1d}}$, $I_2(s) = -\frac{Z_s(s)\,.\,I_s(s)}{R_2/s + jX_{2d}}$, $V_s = \frac{U}{\sqrt{3}}$, $\frac{1}{Z_p} = \frac{1}{jX_m} + \frac{1}{R_1/s + jX_{1d}} + \frac{1}{R_2/s + jX_{2d}}$

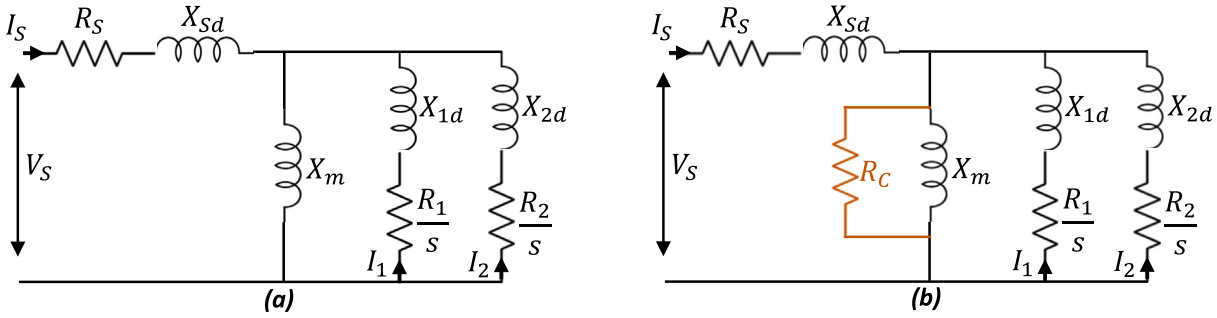

Fig. 3. Double cage model, (a) model developed in [18], (b) proposed model with core loss resistance.

Table 2
132 kW 380 V 50 Hz 4P datasheet.

Output	Poles	Frequency	Rated Voltage	Rated current	LR current(p.u)	Rated speed	Rated torque	LR Torque (p.u)	Breakdown torque(p.u)
132 KW	4	50 Hz	380/660 V	233/134A	1608/926A	2375 rpm	424 Nm	1.8	2.8

Table 3
Experimental Electrical Equivalent Circuit Parameters.

R_S	X_S	R_c	X_m	R_1	X_{1d}	R_2	X_{2d}
0.0053	**0.0673**	**30.818**	**2.3522**	**0.0107**	**0.1305**	**0.0834**	**0.0673**

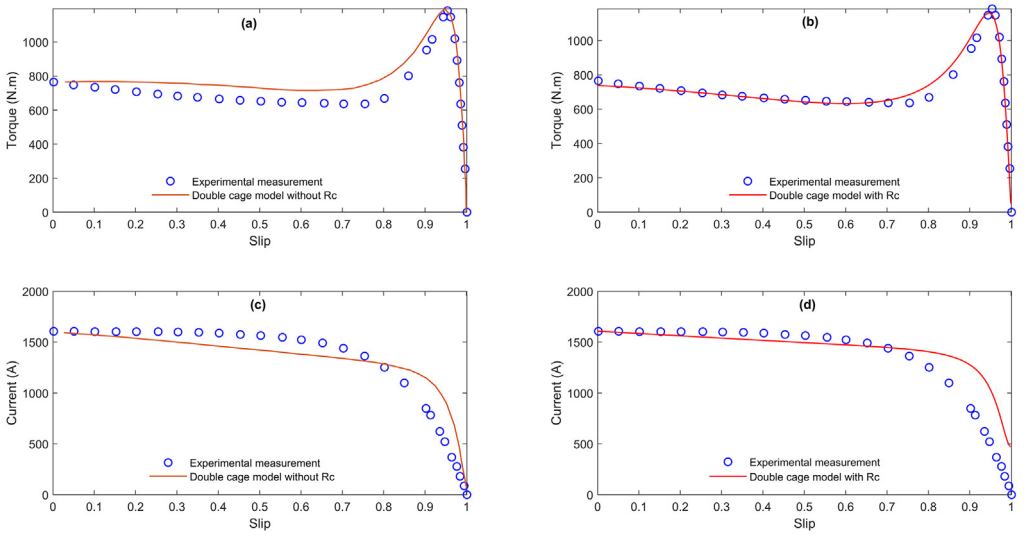

Fig. 4. Comparative Analysis of Double Cage Model (Figure 3) and Experimental Data using Torque-Slip Curves (a) & (b) and Current-Slip Curves (c) & (d)

Table 4
SCIM losses expressions.

LOSSES	Equation	Parameters expressions	Validation	Note
Stator Copper	$\boldsymbol{R_S} \times (\boldsymbol{I}_{s1}^2 + \boldsymbol{I}_{s2}^2 + \boldsymbol{I}_{s3}^2)$	$R_S = R_{Sref} \times [1 + \alpha_{copper}(T - T_{ref})]$	[41,42]	***Inputs:***
Stator & rotor core	$R_C \times (\boldsymbol{I}_{C1}^2 + \boldsymbol{I}_{C2}^2 + \boldsymbol{I}_{C3}^2)$	$R_C = R_{Cref} \times [1 + \alpha_{copper}(T - T_{ref})]; I_C = \frac{V_S - (R_S + jX_S)I_S}{R_C}$	[42]	• *T: Internal estimated temperature in RT*
Rotor cage	$R_r \times (\boldsymbol{I}_{r1}^2 + \boldsymbol{I}_{r2}^2 + \boldsymbol{I}_{r3}^2)$	$R_r = R_{rref}\left[\left(\frac{R_1}{s} + jX_1\right) // \left(\frac{R_2}{s} + jX_2\right)\right] @ T_{ref}$	[41,42]	• ω_r*: Rotor speed measured using the tachometer*
				• f_S*: Stator frequency collected from the* ***VFD***
				• V_S: Stator voltage collected from the sensor
		$I_r = \frac{V_S - (R_S + jX_S)I_S}{Z_r}$; $Z_r = R_r + j\,X_r$		• I_S: Stator current collected from the sensor***Parameters extract***
Mechanical (Windage and friction)	$K_{fw}.P_{in}$	$K_{fw} = \begin{cases} 2.5\%for2poles \\ 1.2\%for4poles \\ 1\%for6poles \\ 0.74\%for8poles \end{cases}$	[32]	***from experiments & optimization forECPs:*** • T_{ref} *: T is the reference temperature (25 °C)* • R_{Xref} : Is the X resistance @ the experiment temperature,X = {stator, core, 1st rotor cage, 2nd rotor cage}, • X_X: Is the X reactance determined by the ECPs extractionX= stator, core, 1st rotor cage, 2nd rotor cage, • α_Y: Temperature coefficient for Y material @ T. α_{copper} = 0.004/°C, and $\alpha_{aluminium}$ = 0.0043 °C [41] • α_Y:Temperature coeficiant for Ymaterial @ Texp • *m&n*: Evaluated by non linear regression [10] • K_{fw}: Friction and windage coefficient. ***Parameters determined by optimization for EE:****CF*: Correction factor
Stray	$\boldsymbol{K}_{stray} \times \boldsymbol{P_{out}}$	$\boldsymbol{K}_{stray} = \left(\frac{L_{fs}}{p.L_m}\right)^{\boldsymbol{m}} \left(\frac{L_r}{p.L_m}\right)^{\boldsymbol{n}} \boldsymbol{L_S} = \frac{X_S}{2\pi f_S}; \boldsymbol{Lm} = \frac{X_m}{2\pi f_S}; \boldsymbol{L_r} = \frac{X_r}{\omega_r}$	[22,10,43]	
Correction factor	$CF.\boldsymbol{P_{totallosses}}$	$CF = [\boldsymbol{cf}_{5,1}]$	–	

Based on the chosen double cage model and the limitation of the in-situ aspect, the expressions of the losses are developed by (Table 4) taking into account the following assumptions:

- The internal temperature of the motor is assumed to be linear during the operation,
- When the motor is off, its temperature is considered to be equal to the ambient temperature, which is assumed to be 25 degreesC. When running, the motor's temperature increases and is assumed to be the same for the stator and the rotor.
- The input voltages and currents are perfect sine, and are out of phase by $2\pi/3$ *rad*,
- The friction and windage coefficient for 8 pole-pair motors is estimated by 4-degree polynomial interpolation of the pole-pair in function of the friction and windage coefficient ($p = f(K_{fw})$) function.
- The stray loss model exponents n and m are assumed to not change for the motor of pole pairs beyond the value of 3.

The temperature dependency.

The steady-state operation of the motor through the DS is run by the proposed hybrid model where the dynamics are ensured by the input power (especially voltage, current, and power factor), the internal temperature, and the shaft speed. The temperature is assumed to vary linearly with the resistances when the motor operates. The guiding coefficient of the temperature is determined using the following equation established by cold and hot DC tests[3] to determine the stator, rotor, and core loss resistances [40].

$R_{ho} = \frac{R_{co}(T_{ho} + k_1)}{T_{co} + k_1}$=> T_{ho}, and the temperature varying is modeled by $T(t) = \frac{T_{ho} - T_{co}}{\Delta t} \times t + T_{co}$ (2).

The choice of the using stray loss model results from a review and comparison of three state-of-the-art stray loss models ([10,43,44]) in [22]. The using SL model is proposed and selected among 6 improved candidate models (referred to in Table II of [10]). In the mentioned previous paper, the exponents are estimated by a 5-fold cross-validation method with standard deviation where the SL experimental data of 18 motors with 1,2,3 pole pairs are subdivided into 5 sub-samples where 4 sub-samples are used as training datasets and the rest for the test dataset. The estimated exponents vary in function of the number of pole pairs, so to reduce this variation, the number of pole pairs is included in the models (referred to Table III), and the exponents are then evaluated using the same procedure. In the end, the model is selected by using Akaike Information Criterion (BIC) and Bayesian Information Criterion (BIC) based on the residual sum of squares SL [10].

The exponents m and n do not vary with the number of pair poles as can be seen in Table 5.

$$\eta = \frac{P_{out}}{P_{in}} = \frac{P_{in} - P_{total\ losses}}{P_{in}}$$

$$P_{total\ losses} = P_{sj} + P_c + P_{rj} + P_m + P_{stray} \quad (3)$$

The global form of the proposed EE equation is $\eta = 1 - CF.f(ECPs).\boldsymbol{P_{out}}$, where f = $f(ECPs) = \frac{P_{total\ losses}}{P_{in}}$is in function of the ECPs, and *cf* is 5 rows, 1 column matrix for (Table 6) losses values correction, it is estimated by optimization.

The correction (Table 7) factors are added to the Energy efficiency model to take into consideration the losses estimation shortcoming, such as:

[3] The resistance of the windings is calculated when the motor is cold (ambient temperature). the motor is then run to 100% of its operating load for 1 h, then the resistance of the stator windings is measured again under these conditions. The difference between the temperatures of each resistance during 1h represents the leading coefficient of the linear affine model of the temperature.

Table 5
Exponent m, and m value from the selected stray loss model [10].

Pole pairs\Exponents	m	n
1	0.95	0.33
2	0.95	0.34
3	0.95	0.34

- The rated energy efficiency is not used in the standard experimental data formulation problem
- The energy efficiency model is highly non-linear, and the loss expressions containing the residual error were compared w.r.t the experimental data in the validation step. These models are validated from different environments.
- Insulation and bearing losses are not taken into account in the EE model.

4.2. Using the ANFIS model for ECPs prediction

The ANFIS model is a hybrid algorithm that combines fuzzy logic and an artificial neural network, which is used to model nonlinear functions, identify nonlinear components online in a control system, and predict a chaotic time series, all yielding remarkable results [45]. It is a powerful approach for modeling nonlinear and complex systems with less input and output training data of the studied system. This advantage is due to the combination of the ANN capability in learning from processes and the Fuzzy logic control capability in handling uncertain information. This makes ANFIS capable of approximating nonlinear and uncertain systems without requiring a purely mathematical model. In addition, the ANFIS algorithm requires less training data. The ANFIS architecture is a multilayer feed-forward (FF) network that is the result of the combination of fuzzy logic and an Artificial neural network (ANN). Based on the experimental input and output data, an ANN uses the input and the output data to learn the system behavior, apply the correct rules, and assign the correct membership function values to obtain the best performance.

In the case of a fuzzy inference system, which consists of two inputs $\times$ and y, each input has two related membership functions (MFs), as shown in Fig. 5. The system also has one output, denoted by f. The output of a first-order Takagi-Sugeno FIS, comprising two IF-THEN rules, can be expressed as follows [46]:

$$\text{1st rule}: \ \textit{if } x \textit{ is } D_1 \textit{ and } y \textit{ is } C_1, \ \textit{then } g_1 = \alpha_1 x + \beta_1 y + \gamma_1, \tag{4}$$

$$\text{2nd rule}: \textit{if } x \textit{ is } D_2 \textit{ and } y \textit{ is } C_2, \ \textit{then } g_2 = \alpha_2 x + \beta_2 y + \gamma_2 \tag{5}$$

Where $\alpha_1, \beta_1, \gamma_1$, and $\alpha_2, \beta_2, \gamma_2$ represent the consequence parameters, and D_1, D_2, C_1, and C_2 are the membership functions (MFs). The ANFIS is consisting of five layers, with it consisting of a wide range of inputs, and just one output is elaborated as follows:

Table 6
Induction motors manufacturer data.

p	$P(KW)$	$Cos\varphi_{FL}$	T_M/T_{FL}	T_{ST}/T_{FL}	I_{ST}/I_{FL}	$\omega_{FL}(rpm)$	η_{FL}	p	$P(KW)$	$Cos\varphi_{FL}$	T_M/T_{FL}	T_{ST}/T_{FL}	I_{ST}/I_{FL}	$\omega_{FL}(rpm)$	η_{FL}
6	500	0.87	2.7	2.3	6.5	992	0.966	2	15	0.92	2.9	2.2	6.6	2910	0.904
8	400	0.82	2.6	2.1	6.5	742	0.962	2	14	0.9	1.8	1.6	7	2920	0.82
4	355	0.87	2.7	2.2	6.8	1486	0.967	6	12	0.8	1.8	1.5	6	980	0.86
6	315	0.84	3	2	7.3	991	0.962	2	11	0.9	3.1	2.2	7	2945	0.91
6	250	0.8	3	2.2	7.3	991	0.91	6	10	0.73	1.8	1.5	6	980	0.86
4	200	0.87	2.7	2.7	7	1488	0.962	6	9	0.78	1.8	1.4	6	970	0.85
4	160	0.86	2.7	2.4	7	1487	0.96	6	8	0.74	2.5	2.1	4.6	960	0.86
4	132	0.86	3	2.7	7.2	1486	0.955	4	7.5	0.89	1.8	1.5	6.5	1450	0.84
2	110	0.86	3	2	7.6	2982	0.955	8	7	0.66	1.8	1.5	5.5	730	0.85
4	90	0.86	2.7	2.2	6.8	1480	0.94	4	6.5	0.85	1.8	1.5	6.5	1450	0.84
2	82	0.93	1.8	1.4	7	2970	0.88	6	6	0.73	1.8	1.5	6.0	980	0.85
4	75	0.86	2.4	2.1	6.3	1482	0.947	2	5.5	0.88	1.8	1.6	7	2860	0.79
4	72	0.9	1.8	1.4	6.5	2970	0.91	4	4.5	0.84	1.8	1.5	6.5	1450	0.83
4	60	0.9	1.8	1.4	6.5	1480	0.91	2	4.0	0.88	1.8	1.6	7	2860	0.80
8	55	0.82	2.4	2.2	6	738	0.931	6	3.7	0.73	1.8	1.5	6	970	0.82
8	47	0.81	1.8	1.4	6	740	0.91	4	3.3	0.83	1.8	1.5	6.5	1450	0.81
8	45	0.81	2.3	2.1	6	740	0.92	2	3	0.89	1.8	1.6	7	2800	0.77
6	42	0.87	1.8	1.4	6.5	980	0.9	4	2.8	0.82	1.8	1.3	6.5	1440	0.77
4	37	0.86	3.1	2.5	7	1475	0.929	8	2.6	0.62	1.8	1.5	5.0	730	0.78
4	34	0.9	1.8	1.3	7	1470	0.87	2	2.4	0.9	1.8	1.6	7.0	2850	0.76
4	32	0.89	1.8	1.4	6.5	1480	0.90	4	2.2	0.8	1.8	1.3	6.5	960	0.77
2	30	0.88	2.7	2.3	6	2940	0.91	2	1.8	0.8	1.8	1.6	7.0	2850	0.74
4	28	0.87	1.8	1.3	7	1470	0.87	6	1.5	0.7	1.8	1.4	6	940	0.75
4	26	0.89	1.8	1.4	6.5	1470	0.89	6	1.3	0.7	1.8	1.4	6	940	0.74
6	22	0.77	2.9	2.8	5.5	975	0.908	2	1.1	0.8	1.8	1.6	7.0	2800	0.72
6	20	0.76	1.8	1.5	6	980	0.88	4	0.85	0.79	1.8	1.3	7	1420	0.70
4	19	0.84	3.2	2.7	6.9	1460	0.905	4	0.85	0.8	1.8	1.5	6.5	1430	0.74
4	19	0.88	1.8	1.5	6.5	1470	0.89	2	0.75	0.9	1.8	1.6	7.0	2860	0.66
4	17	0.92	1.8	1.5	7.0	1470	0.87	6	0.65	0.70	1.8	1.40	6.50	920	0.64
4	16	0.85	1.8	1.3	6.5	1470	0.85	2	0.55	0.9	1.8	1.6	7.0	2860	0.65

Table 7
Initial values of the correction factors for efficiency estimation.

cf_1	cf_2	cf_3	cf_4	cf_5	*RMSE*	*Pole − paire*
1.0000	1.0000	0.0091	1.0000	5.0000	0.1046	8
0.9995	0.9874	0.3210	0.9999	4.9996	0.1532	6
0.9996	0.9997	0.0046	1.0000	4.9998	0.1317	4
0.9994	0.9444	0.9998	1.0000	4.9999	0.1753	2

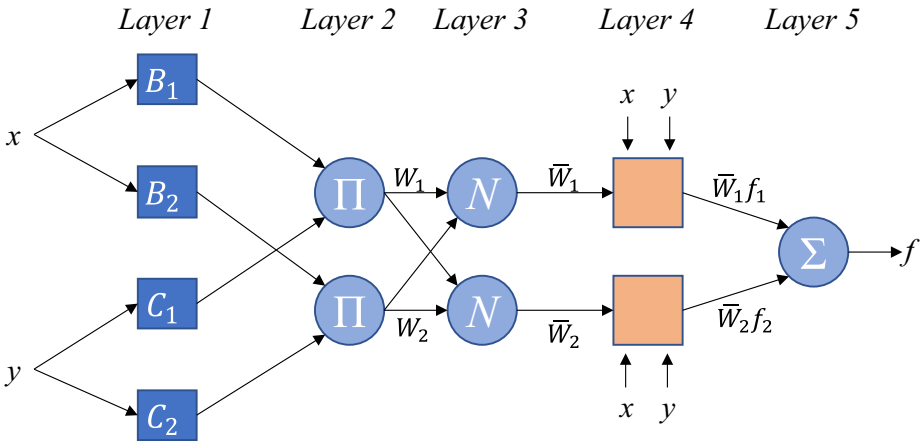

Fig. 5. Adaptive neuro-fuzzy inference (ANFIS) basic architecture with 2 inputs.

Layer 1 (or fuzzification layer): Each node is controlled by a specific, which an input '*x*' satisfies the linguistic concept that is represented by μ_{D_k}.

$$O_k^1 = \mu_{D_k}(x) \tag{6}$$

Where O_k^1 is the layer's output, and $\mu_x(x)$ is a membership function.

Layer 2: Is represented by the fixed nodes ($\prod$) which generate output for instance O_k^2 of each node k.

$$O_k^2 = w_k = \mu_{D_k}(x) \times \mu_{C_k}(y) \tag{7}$$

Where O_k^2 is the layer output, and w_k is the stands for firing strength for the k^{th} rule.

Layer 3: The k^{th} node of this layer computes a normalized firing strength as in layer 2, by the following relation, in which h represents the number of nodes in this layer.

$$O_k^3 = \bar{w}_k = \frac{w_k}{\sum_{k=1}^{h} w_k} \tag{8}$$

Layer 4: This is the defuzzification layer where all nodes of this layer compute a linear function expressed as:

$$O_k^4 = \bar{w}_k g_k = \bar{w}_k(\alpha_k x + \beta_k y + \gamma_k) \tag{9}$$

Layer 5: Computes the output of the network by the following expression:

$$O_k^5 = \sum_k w_k g_k \tag{10}$$

4.2.1. Evaluation of the accuracy of the predicted magnitudes

The accuracy of the predicted ECPs and energy efficiency are assessed by calculating, the root mean square error (RMSE) and the mean absolute error (MAE).

The root mean square error or RMSE is the most commonly used in supervised learning applications as an indicator for the quality of predictions. It shows the deviation between the predictions from the true measured values using Euclidean distance. The mathematical expression of RMSE is shown in (11) as:

$$RMSE = \sqrt{\frac{\sum_i^n (\eta_i - EE_i)^2}{n}} \tag{11}$$

Where η is the experimental value of the efficiency, EE is the predicted value of the efficiency, and n is the total number of observations. It is very important to note that the RMSE is not scale invariant, so if a comparison will be made using this measure, it would be only with a model using the same scale of data.

The MAE is the mean of the amount of the absolute error between the measured EE and its corresponding predicted value, it is used with regression models. The residual absolute errors in MAE are not weighted more or less, but the scores increase linearly with the increase in errors. Hence, as RMSE, this measure is not scaling invariant. The MAE value can be calculated mathematically as in (12):

$$MAE = \frac{\sum_i^n |\eta_i - EE_i|}{n} \tag{12}$$

4.2.2. Experimental data normalization to train the ANFIS models

To develop the proposed model, the data of 60 motors are collected from [15] and from the manufacturer "Hongma Motor", where 85 % of these data are used to train the ANFIS model, and the rest of the data are used to test the model. The ANFIS model is then implemented in SIMULINK and run with the following inputs: starting torque and current, maximum torque, full load slip, efficiency, rated active power, and reactive power in the per-unit system.

To train the ANFIS model from the MATLAB TOOLBOX the experimental input and output data that are used for the training are formulated as follows (Fig. 6): For each motor, the manufacturer data are used to find the ECPs using FSOLVE, and then the EE is calculated from the ECPs and the speed through the proposed EE model. The data provided by the manufacturers in the datasheet are the rated mechanical power, the reactive power, the maximum torque, the starting torque, the full load torque, the starting current, and the full load current. These data are collected from the routine test and allow us to establish 6 equations.

The global form of the equation system is $F(X) = 0$ (manufacturer data – calculated equivalent magnitudes in the per-unit system) and it is expressed as follows:

The problem has 8 parameters but only 6 of them are independent and 3 relations can be added based on the literature [18,19,47]:

- $R_s = K_R R_1, X_{2d} = K_x X_s$, where $R_2 > R_1$ and $X_{1d} > X_{2d}$ (13)

and the case where $K_R = 0.5$ and $K_X = 1$ gives the best performance.

- The maximum torque condition $\frac{dT(S_M)}{dS} = 0$ (14)

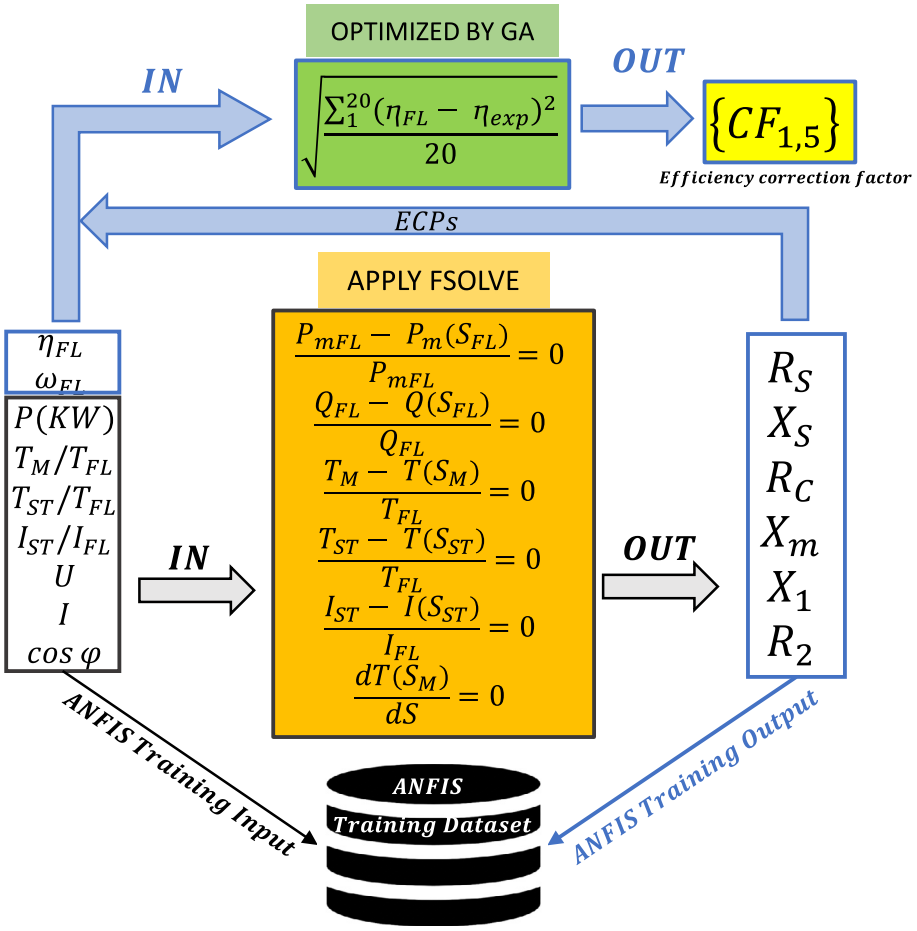

Fig. 6. Flowchart of the proposed data set calculation technique to train the ANFIS model and to optimize the proposed model.

$X = X_s, R_C, X_m, R_1, X_{1d}, R_2$ and $F = f_1 f_2 f_3 f_4 f_5 f_6$

$$f_1(X) = \frac{P_{mFL} - P_m(S_{FL})}{P_{mFL}} = 0$$

$$f_2(X) = \frac{Q_{FL} - Q(S_{FL})}{Q_{FL}} = 0$$

$$f_3(X) = \frac{T_M - T(S_M)}{T_{FL}} = 0 \quad (15)$$

$$f_4(X) = \frac{T_{ST} - T(S_{ST})}{T_{FL}} = 0$$

$$f_5(X) = \frac{I_{ST} - I(S_{ST})}{I_{FL}} = 0$$

$$f_6(X) = \frac{dT(S_M)}{dS} = 0$$

where P_{mFL} is the mechanical full-load power, Q_{FL} is the reactive power, T_M is the maximum power, T_{ST} is the starting torque, I_{ST} is the starting current and η_{FL} is the motor efficiency at full-load conditions.

Equations (15) are solved for each motor in the non-linear system to get the 6 uncorrelated parameters by using the routine fsolve function in MATLAB. It uses a nonlinear least squares algorithm that employs the Gauss-Newton method or the Levenberg-Marquardt method. The advantage of a method based on least squares is that when the solution is not zero, the method behaves like an optimization algorithm, i.e. say it converges to an absolute minimum. The residue (ε) at the converged point can be considered as:

$$\varepsilon = \sum_i f_i \quad (16)$$

Finally, the initial value of the correction factor is estimated at a steady state by applying "fmincon" function from the Matlab optimization toolbox on the RMSE, $\varepsilon = \sqrt{\frac{\sum_1^{20}(\eta_{FL}-\eta_{exp})^2}{20}}$, formed by the 60 motors on 4 categories classified by the number of pole pairs. "fmincon" minimizes an objective function of several variables using the Nelder-Mead algorithm. These initial values can be considered in the EE estimation as the optimal correction factor for each pole-pair when optimization is not possible. To perform the precision of the model, the constraints on the losses are added in the optimization by taking into consideration the rated power and the typical loss share in SCIMs [48].

$$\begin{cases} P_{sj} = 52\%of502W \\ P_c = 4\%of502W \\ P_{rj} = 21\%of502W \\ P_m = 4\%of502W \\ P_{stray} = 4\%of502W \end{cases}$$, Where 502 W represents the rated value of the total loss of 1.5 Kw SCIM.

4.2.3. Training and testing of the ANFIS algorithm using ANFIS MATLAB toolbox

To perform the proposed dynamic model, firstly the ANFIS Matlab function is used, and upload the experimental data for training and testing. Secondly, the SIMULINK FUZZY block function is used with the performed ANFIS output. Thirdly, the SIMULINK block

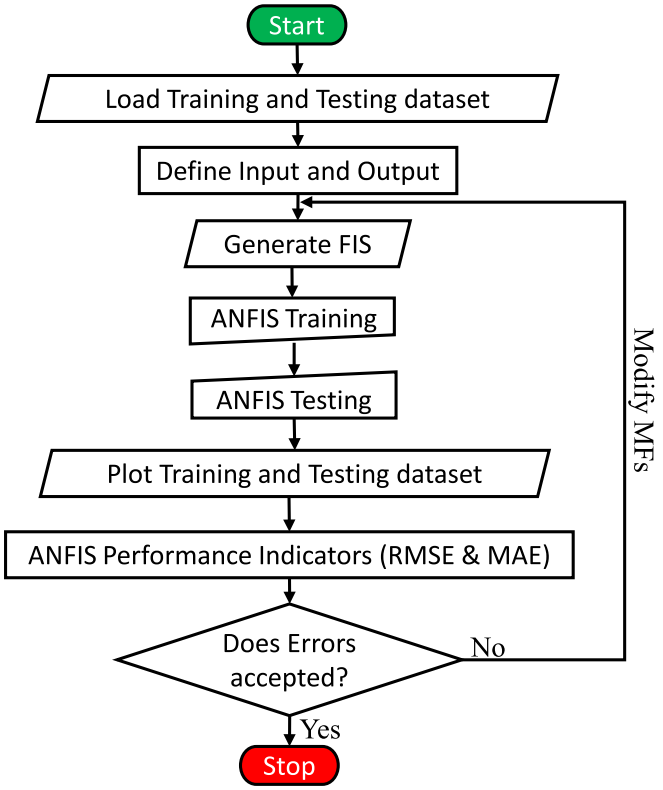

Fig. 7. Training and Testing flowchart of the proposed ANFIS algorithm.

motor with the same characteristic as the testing motor is used to estimate the rotor speed. Finally, the motor efficiency is calculated and monitored by the estimated EECPs and the measured speed. The training and testing process of all ANFIS algorithms is done following the Fig. 7 flowchart.

Two methods are available in MATLAB to train the ANFIS model, the backpropagation gradient descent method as well as the hybrid method. The hybrid algorithm is significantly more efficient in training the ANFIS model, and it improves the robustness of the ANFIS system for both classifications and regression. This is possible because it combines the steepest-descent and the least squares estimate (LSE) algorithms. In many research works, the hybrid method is favored against the gradient descent because it gives optimum results [46,49,50]. Hence, it is the preferred method in this study. The FIS system generation can be obtained using substructure clustering, grid partitioning, and/or Fuzzy C-means clustering (FCM). However, only the two first methods are available in the MATLAB toolbox. Grid partitioning is applied when the number of inputs and their membership functions is small (less than six) [46]. In this study, the sub-clustering algorithm was chosen and applied since the input variables are eight and the simulation time is relatively high. According to the study done in [15], different ANFIS structures are tested to estimate the ECPs of a double cage model. Fig. 9 (b) shows the ANFIS structure of R_S parameter and the best ANFIS configuration is obtained with Matlab' Gaussmf. Hence, the Gaussian one is used for the input and the linear membership function is used for the output. The mathematical expression of the Gaussmf is given by (17).

$$gaussian(x, c, \sigma) e^{-0.5\left(\frac{x-c}{\sigma}\right)^2} \tag{17}$$

Where σ presents the curve's width, and c, the center location.

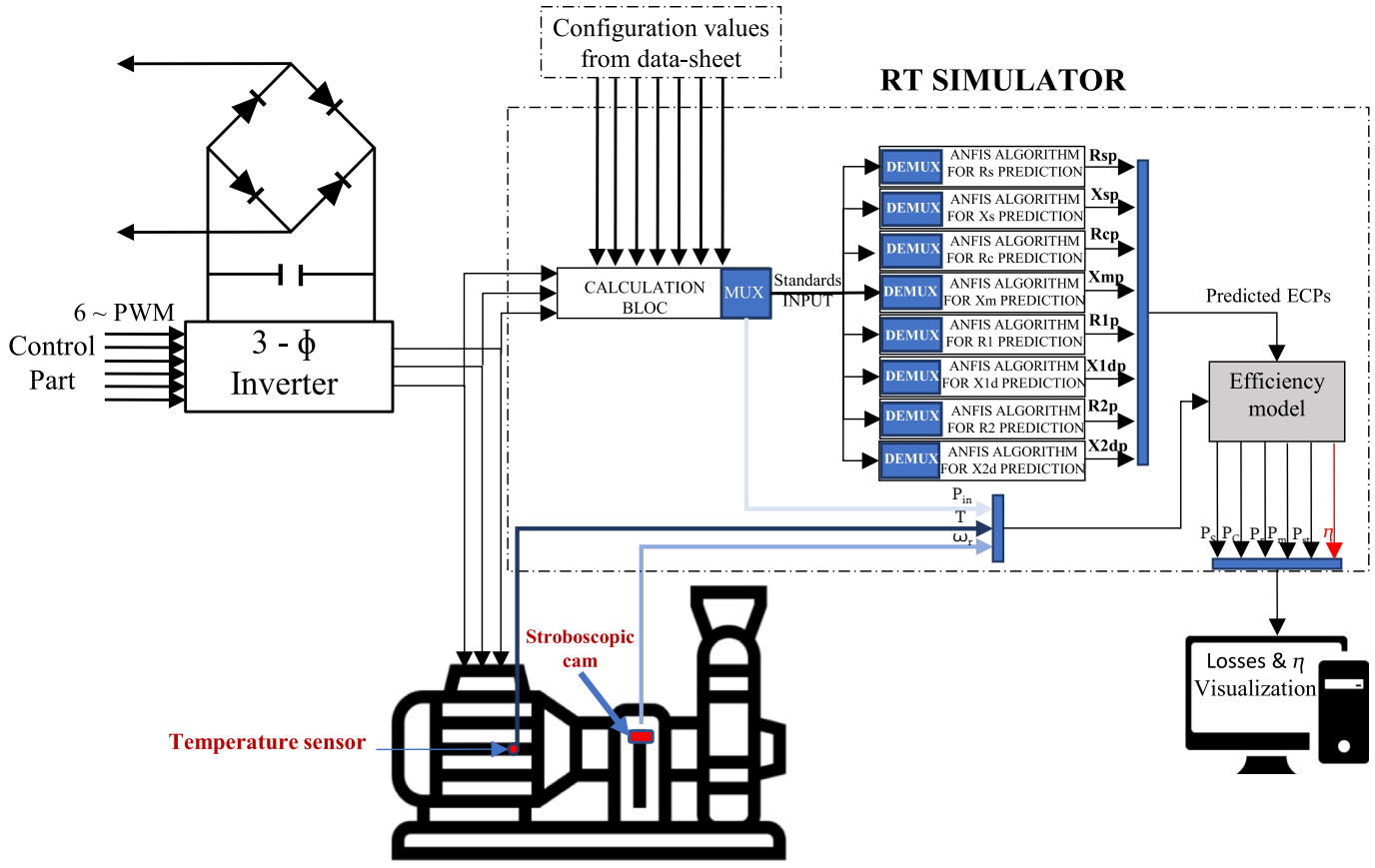

Fig. 8. The Simulation diagram of the proposed method for RT in-situ EE and losses estimation.

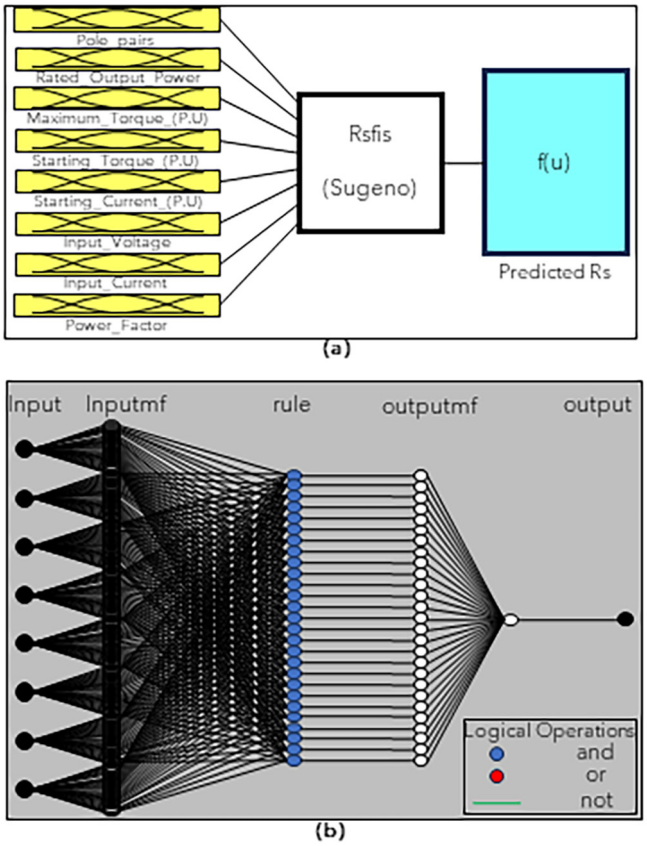

Fig. 9. Rs FIS designer (a), Rs parameter ANFIS structure with 27 rules (b).

5. Results and discussions

The proposed model has been validated using SIMULINK, where the test bench shown in Fig. 8 has been simulated with experimental data. The validation involves plotting and comparing the efficiency results obtained from the proposed model with those obtained from measurements of a 1.5 kW, 230/400 V 50 Hz motor. In addition, torque, and losses have been monitored during the simulation, and this section describes also the performance results obtained using optimal ANFIS algorithms. The experiments demonstrate the effectiveness of the proposed approach.

To evaluate the performance of the proposed ANFIS algorithm, RMSE and MAE are calculated during the training and testing process. Fig. 10, and Fig. 11 show respectively the training and the testing comparison between the experimental ECPs calculated by the numerical method, and the estimated ECPs estimated by the ANFIS method. Most of the studies that tackled the double cage ECPs estimation used the double cage with 7 parameters [15]–[20,47]. However, the double cage model with 7 parameters can give good results but the accuracy of the model with 8 parameters is higher. This confirms that by having more parameters, the accuracy is higher for both linear and non-linear models [18]. The work done in [15] applies the ANFIS model to estimate the 7 parameters of a double cage Induction motor with the following results: the mean of the RMSE and the MAE of the estimated ECPs are 7.855e-5 and 5.54e-05 respectively for training and 0.017 and 0.012 for testing. The work done in[16] uses also the ANFIS algorithm to estimate 7 ECPs whit a mean relative error of 5.6%. Table 8 shows the specification of the optimal using ANFIS model for each parameter, and also presents the errors during the training and the testing process, while, Fig. 11 shows the Taylor diagram of each parameter (Fig. 12).

5.1. The IM EE-based DS: EE monitoring

This simulation aims to highlight the proposed method where simulation is done as follows:

- Neuro-Fuzzy Designer from MATLAB toolbox is used in a SIMULINK block function to estimate in RT the ECPs based on the training described in section 4.2.3. This algorithm is run by measuring voltage, current, and power factor as dynamic input, and also the normalized data from the motor manufacturer datasheet is considered as static input.

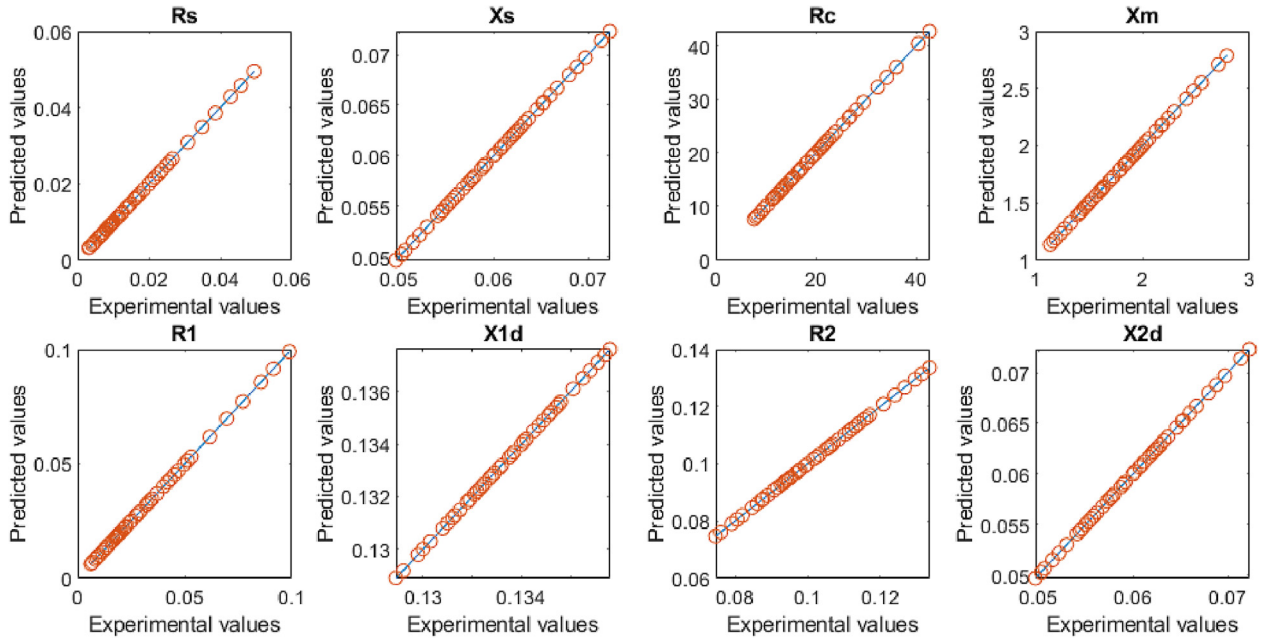

Fig. 10. Comparison of the predicted ECPs estimated with the ANFIS Algorithm w.r.t the calculated ECPs experimentally for Training data.

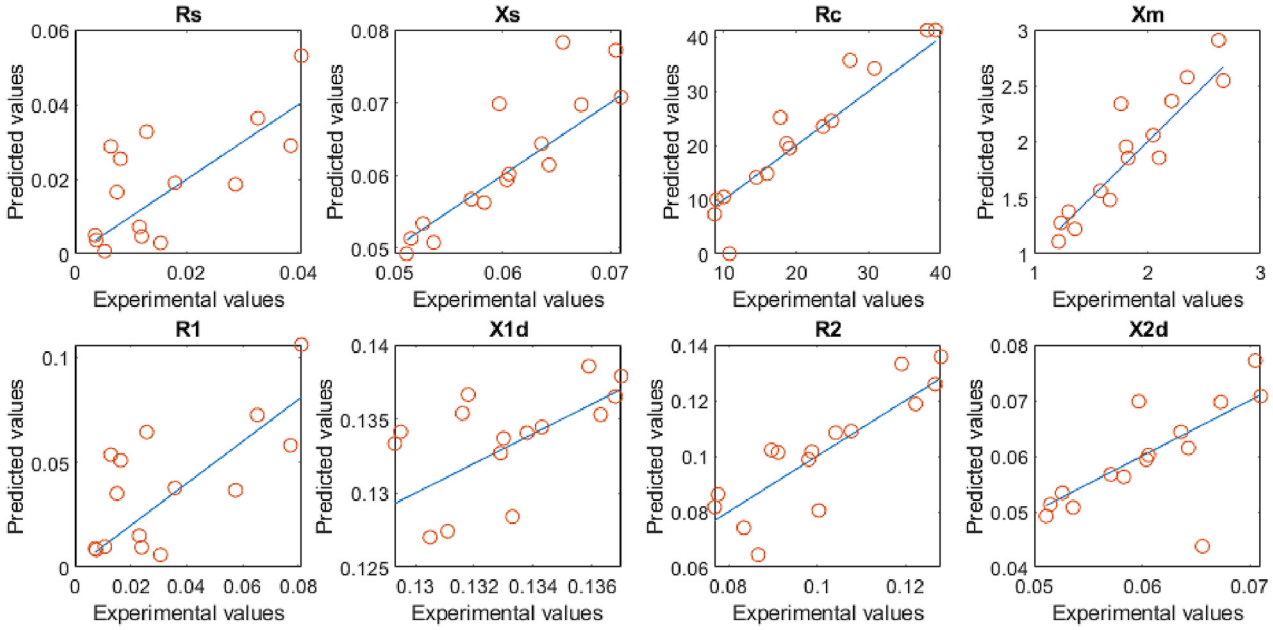

Fig. 11. Comparison of the predicted ECPs estimated with the ANFIS Algorithm w.r.t the calculated ECPs experimentally for Testing data.

Table 8
Parameters specification of the used ANFIS MATLAB model.

Specification	R_S	X_S	R_C	X_m	R_1	X_{1d}	R_2
Type	Sugeno	Sugeno	Sugeno	Sugeno	Sugeno	Sugeno	Sugeno
Input/Output	8/1	8/1	8/1	8/1	8/1	8/1	8/1
Input membership function type	Gaussmf	Gaussmf	Gaussmf	Gaussmf	Gaussmf	Gaussmf	Gaussmf
Output membership function type	Linear	Linear	Linear	Linear	Linear	Linear	Linear
No. of fuzzy rules	27	36	32	35	29	35	35
No. of nonlinear parameters	432	576	512	560	464	560	560
No. of linear parameters	243	324	288	315	261	315	315
No. of epoch	2	2	2	2	2	2	2
Minimal training RMSE	1.02e-07	9.29e-07	0.00048364	0.00011498	1.71e-07	3.22e-06	1.68e-06
Minimal testing RMSE	0.01695283	0.0047671	4.26807045	0.20812817	0.03319269	0.00299727	0.04000779
Minimal training MAE	7.37e-08	3.71e-07	0.00013253	2.94e-05	1.22e-07	1.17e-06	6.41e-07
Minimal testing MAE	0.01162112	0.00302326	2.81700507	0.1564502	0.02240477	0.00236709	0.0167639

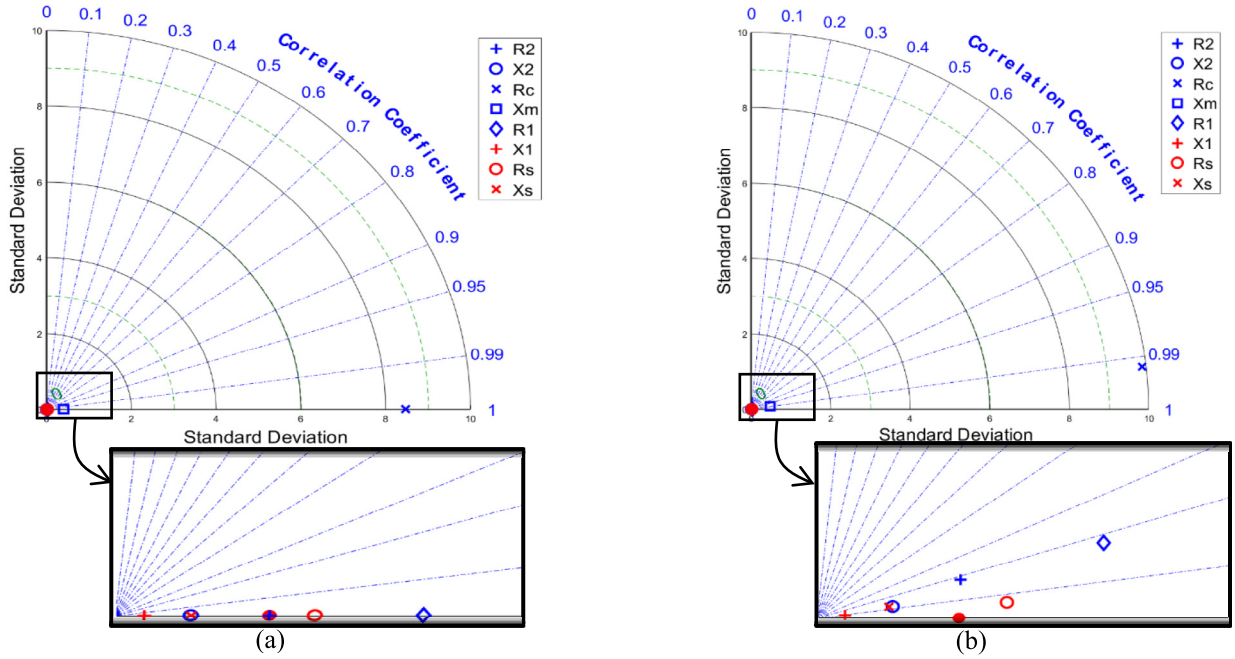

Fig. 12. Taylor diagram of the proposed model for the estimation of ECPs of IMs in the training (a) and the testing (b) stage.

- Then the EE bloc function is programmed using the Simulink block function, where the model is run by the input power, rotational speed, temperature profile, the optimized correction factors, and the ECPs provided from ANFIS Block every 0.5 s,
- From the experiment, the EE data is interpolated by a polynomial of 3 degrees in the speed interval respectively from 1350 to 1301 rpm for linear control.
- The temperature variation is also used in the proposed method as described in the last paragraph of section 4.1.
- The simulation is run for 1 s, and the speed control is used as the mechanical input. The linear, and non-linear speeds are used, but only the EE for the linear speed and torque control are compared w.r.t the measured EE.

At each variation of the speed, the system passes from a transient state before it stabilized. This transition includes an excess of energy consumption, hence decreasing the efficiency. This excess of energy consumption at each speed variation is a good indicator of the fidelity of the proposed model to the physical IMs.

In addition to the transient state, the proposed method accurately predicts the motor EE as shown in Fig. 16 (a). During the simulation of a 1.5 kW SCIM with linear and nonlinear speed inputs (Fig. 13), the dynamic behavior of the torque and losses are depicted in Fig. 14 and Fig. 15, respectively. The magnitude visualization for the linear input shows a certain degree of stability because the varies changes slowly. However, for the nonlinear speed input, significant variation is observed, resulting in energy

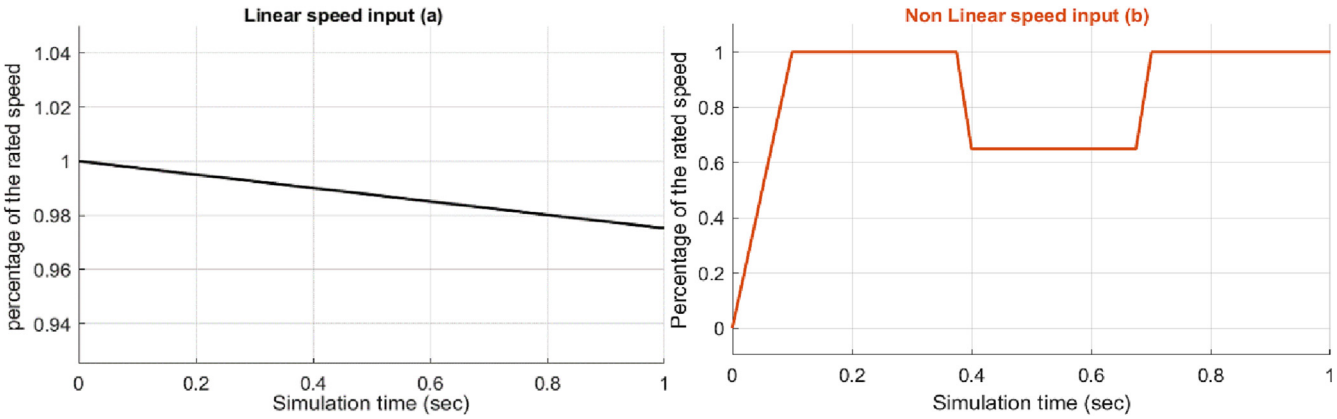

Fig. 13. Speed input profiles.

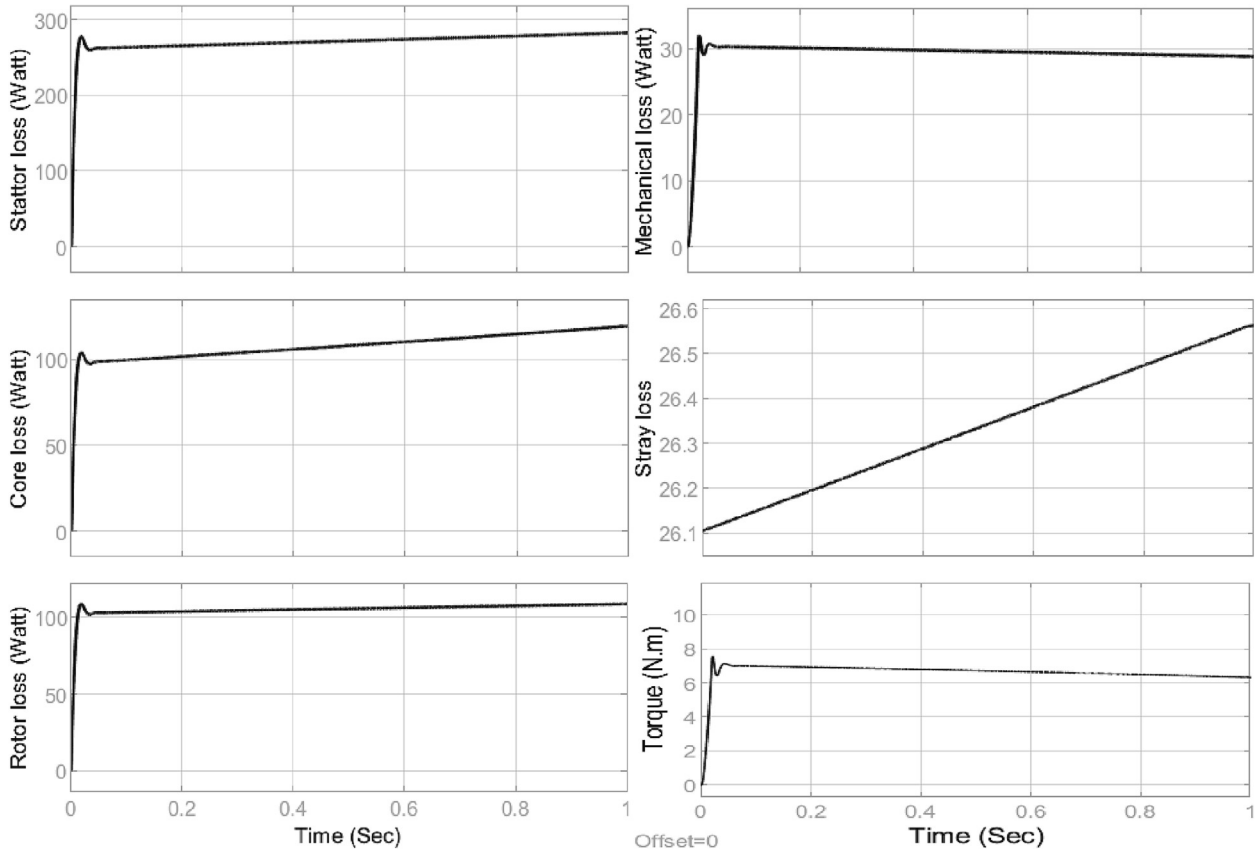

Fig. 14. Losses & torque visualization for linear speed input.

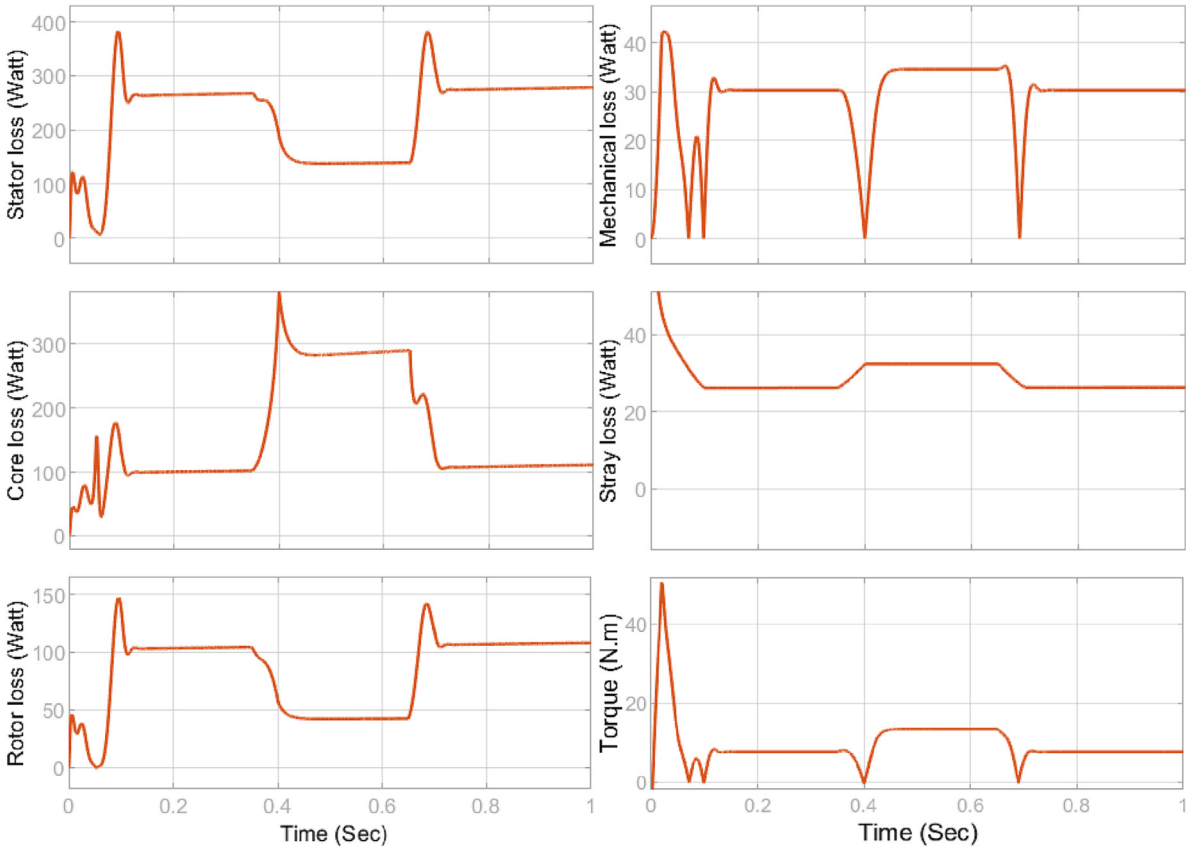

Fig. 15. Losses and torque visualization for non-linear speed input.

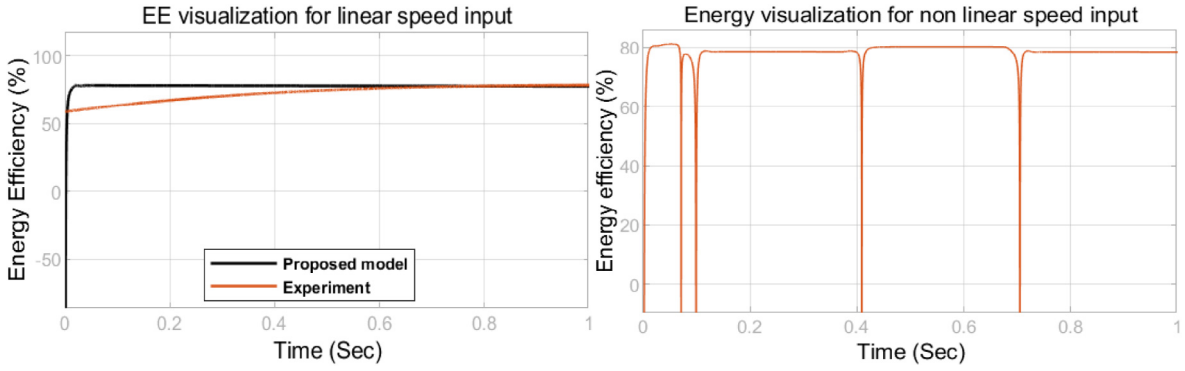

Fig. 16. Energy efficiency visualization for linear and non-linear speed input.

Table 9
The estimated error of the EE calculated with the proposed method w.r.t the measured EE of the 1.5 KW SCIM for linear speed input.

Data	Method	Output	MAE	RMSE
Experimental	Proposed EE model	η	0.1671	0.205

losses with each speed variation, as depicted in the EE visualization. The errors obtained using the proposed method w.r.t the measured EE for the linear speed input are presented in Table 9.

5.2. Toward the implementation of the proposed method

The implementation of the proposed method in a real-world industry must necessarily pass through the offline simulation, then the HIL implementation on a laboratory scale, and finally, the deployment in a real-world industry for a proof of concept. The RT applications are generally used in industries for time-critical systems. The hardware used in RT applications is embedded devices with I/O ports that interface with the physical world and allow control. These systems are characterized by the pre-set time which is the time to read the input signals, make all the calculations by using the model, and generate the corresponding outputs.

In the offline simulation, the time between the beginning to the end of the simulation corresponds to the "step size", but it's not always the same as the time cost to solve the model, hence in MATLAB, the Simulink profiler allows the calculation of the simulation execution time which is the time budget to solve a specific model. In this study, the simulation step size is 1 s, and the simulation execution time of all blocs in the simulation is 3607.942 s, but the proposed model computation time corresponds to the total time to execute the ANFIS parameters estimator bloc, the EE and losses estimation bloc, and the temperature estimator. Table 10, shows the computation time of the proposed model.

With the development of CPU and floating-point numerical signal processing technologies, the devices used in the RT application have been replaced with RT simulators. The most used RT-simulators in the industry are Opal-RT, Typhoon HIL, and MicroLabBox (d-SPACE) [51]. The HIL implementation is simple and requires, RT-simulation software, hardware devices from physical components such as an induction motor with variable load, input power supply with variable frequency drive, temperature and speed sensors, and finally a RT-simulator. The HIL system would be considered by using the RT-simulation hardware and software that can interact with the Simulink model. The well-known software used in this field is RT-Lab which has revolutionized the way Model-based Design is performed. Its flexibility and scalability allow it to be used in virtually any simulation or control system application, and to add computing power to simulations, where and when it is needed. Opal-RT hardware is considered based on the SETB of the proposed method. Fig. 17 test bench is proposed to implement the HIL of the proposed method. In addition to the hardware mentioned earlier, other types of hardware are also used. For instance, in [14], the proposed drive system was modeled and designed using MATLAB software, and then evaluated in a real-time hardware setup using a DSP TMS320F2812 processor.

6. Conclusion

The use of Squirrel Cage Induction Motors (SCIMs) in massive quantities has captured the attention of researchers and industrialists to build more efficient motors and operate them more efficiently. This cannot be achieved without an accurate estimation of the motor energy efficiency (EE) in Real-Time (RT) and in situ. The RT EE and losses estimation allows the collection of historical data which can be used to predict the machine's state of health. Due to the need for accurate EE information, the paper proposes an improved method for DS implementation of the SCIM based on the double cage model with core loss resistance and stray losses. 8 MATLAB ANFIS models are trained and tested to predict the 8 proposed double cage parameters where used the EE model to estimate the motor losses and energy efficiency. 60 SCIMs with rated power between 500 KW and 0.45 KW are used to train and test the using ANFIS model. Among the dataset, 85% of the total data are used for training while the remaining 15% of the total data was used for testing. In addition to the predicted Electric Circuit Parameters (ECPs), the speed, and internal temperature are used to predict five losses incurring in the machine (stator/rotor, core, friction/windage, and stray). A good estimation of these losses produces an accurate assessment of the EE of the motor. As the EE-rated value is not used in the experimental data of the ECPs generation process, correction factors are added to each loss and found by optimizing the RMSE formed by the predicted EE and the rated EE from the manufacturer data. To validate the proposed method, a 1.5 KW SCIM EE was measured in the laboratory and interpolated

Table 10
The computation time of the proposed method using the Simulink profile.

Bloc	ANFIS ECPs Estimator	Rsfis	Xsfis	Rcfis	Xmfis	R1fis	X1fis	R2fis	X2fis	Temperature estimator	Losses & EE estimator
Self-time (sec)	0	0	0	0	0	0	0	0	0	0	0.032
Total time (sec)	2867.440	353.712	381.641	346.422	362.250	352.517	355.913	353.630	361.355	0.19	0.131

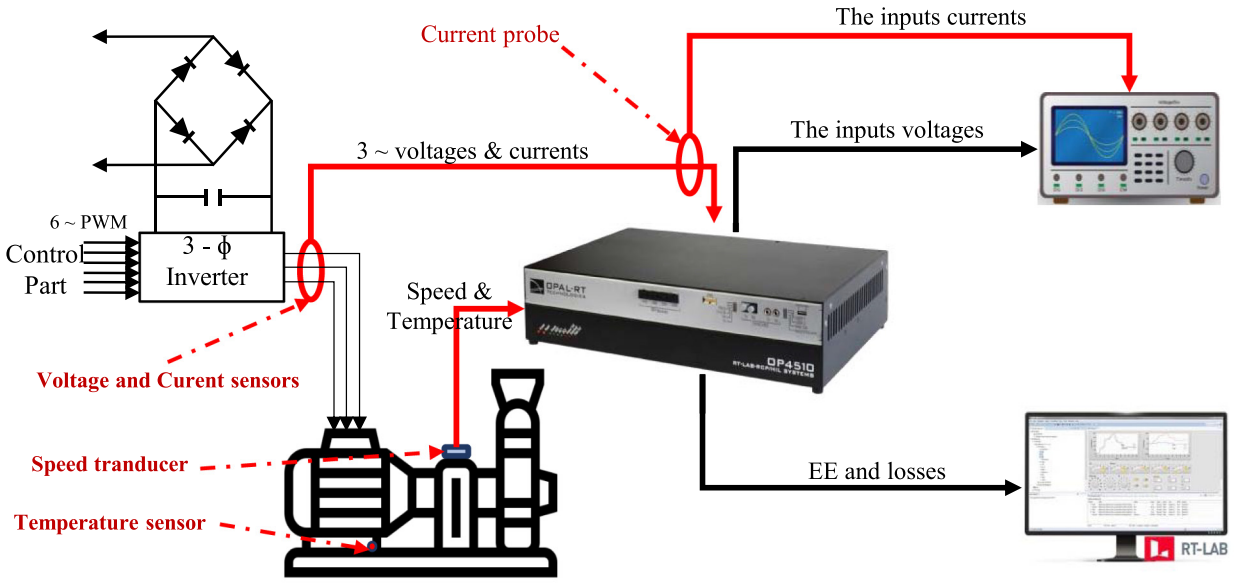

Fig. 17. Proposed Hardware setup for the HIL implementation.

with a 3-degree polynomial to be compared w.r.t the predicted EE through simulation on the SIMULINK environment. The results of the simulations show that the estimated EE is in good agreement with the measured EE with an RMSE of 0.205 for linear speed input. The method gives better accuracy because of its capability to adapt to linear and non-linear control.

7. Perspective for future work

The simulation of the proposed model shows good results on the losses and EE estimation for the linear speed input, and they can be used for (1) a better design of the machine and (2) Energy efficiency-based predictive maintenance. However, the proposed model can include the following developments: The model cannot be implemented in certain industries because of the speed measurement. In this paper, we suggest the use of the stroboscopic-based method to measure the speed, but some industrial structures cannot allow using these techniques. Hence, to get a complete in-situ method, the model speed input can be predicted using speed estimation techniques such as sliding mode observer.

- By having an accurate estimation of each loss in real-time (as in Fig. 14 and Fig. 15). The electrical machine designers could use this information to better identify the parameters that contribute the most to the reduction of the motor's efficiency and hence to the decay of the machine.

Declaration of Competing Interest

The authors declare that they have no known competing financial interests or personal relationships that could have appeared to influence the work reported in this paper.

References

[1] J. Lee, B. Bagheri, H.-A. Kao, A Cyber-Physical Systems architecture for Industry 4.0-based manufacturing systems, Manufact. Lett. 3 (Jan. 2015) 18–23, https://doi.org/10.1016/j.mfglet.2014.12.001.

[2] R.Y. Zhong, X. Xu, E. Klotz, S.T. Newman, Intelligent Manufacturing in the Context of Industry 4.0: A Review, Engineering 3 (5) (Oct. 2017) 616–630, https://doi.org/10.1016/J.ENG.2017.05.015.

[3] R. Walawalkar, S. Fernands, N. Thakur, K.R. Chevva, Evolution and current status of demand response (DR) in electricity markets: Insights from PJM and NYISO, Energy 35 (4) (Apr. 2010) 1553–1560, https://doi.org/10.1016/j.energy.2009.09.017.

[4] K. Bunse, M. Vodicka, P. Schönsleben, M. Brülhart, F.O. Ernst, Integrating energy efficiency performance in production management – gap analysis between industrial needs and scientific literature, J. Clean. Prod. 19 (6) (Apr. 2011) 667–679, https://doi.org/10.1016/j.jclepro.2010.11.011.

[5] H. P. Inamdar and R. P. Hasabe, "It based energy management through demand side in the industrial sector," in *Communication and Energy Conservation 2009 International Conference on Control, Automation*, Jun. 2009, pp. 1–7.

[6] A. Ladj, Z. Wang, O. Meski, F. Belkadi, M. Ritou, C. Da Cunha, A knowledge-based Digital Shadow for machining industry in a Digital Twin perspective, J. Manuf. Syst. 58 (Jan. 2021) 168–179, https://doi.org/10.1016/j.jmsy.2020.07.018.

[7] M. Landherr, U. Schneider, T. Bauernhansl, The Application Center Industrie 4.0 - Industry-driven Manufacturing, Research and Development, Procedia CIRP 57 (Jan. 2016) 26–31, https://doi.org/10.1016/j.procir.2016.11.006.

[8] "4E_2017_Annual_Report_100518.pdf." Accessed: Nov. 01, 2021. [Online]. Available: https://www.iea-4e.org/wp-content/uploads/publications/2018/05/4E_2017_Annual_Report_100518.pdf.

[9] P. Waide, C. U. Brunner, "Energy-Efficiency Policy Opportunities for Electric Motor-Driven Systems," OCDE, Paris, May 2011. doi: 10.1787/5kgg52gb9gjd-en.

[10] R. Kumar, P. Kumar, T. Kanekawa, K. Oishi, Stray Loss Model for Induction Motors With Using Equivalent Circuit Parameters, IEEE Trans. Energy Convers. 35 (2) (Jun. 2020) 1036–1045, https://doi.org/10.1109/TEC.2020.2964616.

[11] H. M. Mzungu, A. B. Sebitosi, and M. A. Khan, "Comparison of Standards for Determining Losses and Efficiency of Three-Phase Induction Motors," in *2007 IEEE Power Engineering Society Conference and Exposition in Africa - PowerAfrica*, Johannesburg, South Africa: IEEE, Jul. 2007, pp. 1–6. doi: 10.1109/PESAFR.2007.4498051.

[12] A. Amadou Adamou, C. Alaoui, Energy Efficiency Model-Based Predictive Maintenance for Induction Motor Fault Prediction Using Digital Twin Concept, in: S. Motahhir, B. Bossoufi (Eds.), Digital Technologies and Applications, Springer Nature Switzerland, Cham, 2023, pp. 600–610, https://doi.org/10.1007/978-3-031-29860-8_61.

[13] M.K. Masood, W.P. Hew, N.A. Rahim, Review of ANFIS-based control of induction motors, J. Intell. Fuzzy Syst. 23 (4) (Jan. 2012) 143–158, https://doi.org/10.3233/IFS-2012-0502.

[14] R.N. Mishra, K.B. Mohanty, Real time implementation of an ANFIS-based induction motor drive via feedback linearization for performance enhancement, Eng. Sci. Technol. Int. J. 19 (4) (Dec. 2016) 1714–1730, https://doi.org/10.1016/j.jestch.2016.09.014.

[15] M.A. Jirdehi, A. Rezaei, Parameters estimation of squirrel-cage induction motors using ANN and ANFIS, Alex. Eng. J. 55 (1) (Mar. 2016) 357–368, https://doi.org/10.1016/j.aej.2016.01.026.

[16] O. Çetin, A. Dalcalı, F. Temurtaş, A comparative study on parameters estimation of squirrel cage induction motors using neural networks with unmemorized training, Eng. Sci. Technol., Int. J. 23 (5) (Oct. 2020) 1126–1133, https://doi.org/10.1016/j.jestch.2020.03.011.

[17] J. Pedra, Estimation of typical squirrel-cage induction motor parameters for dynamic performance simulation, IEE Proceed.-Generat., Transm. Distribut. 153 (2) (2006) 137–146.

[18] J. Pedra, I. Candela, L. Sainz, Modelling of squirrel-cage induction motors for electromagnetic transient programs, IET Electr. Power Appl. 3 (2) (Mar. 2009) 111–122, https://doi.org/10.1049/iet-epa:20080043.

[19] J. Pedra, F. Corcoles, Estimation of induction motor double-cage model parameters from manufacturer data, IEEE Trans. Energy Convers. 19 (2) (Jun. 2004) 310–317, https://doi.org/10.1109/TEC.2003.822314.

[20] P. Pillay, R. Nolan, T. Haque, Application of genetic algorithms to motor parameter determination for transient torque calculations, IEEE Trans. Ind. Appl. 33 (5) (Sep. 1997) 1273–1282, https://doi.org/10.1109/28.633806.

[21] Q. Qi, F. Tao, T. Hu, N. Anwer, A. Liu, Y. Wei, L. Wang, A.Y.C. Nee, Enabling technologies and tools for digital twin, J. Manuf. Syst. 58 (2021) 3–21.

[22] A. A. Adamou and C. Alaoui, "Towards the Implementation of a Digital Twin for Induction Motors," in *Digital Technologies and Applications*, S. Motahhir and B. Bossoufi, Eds., in Lecture Notes in Networks and Systems. Cham: Springer International Publishing, 2022, pp. 513–523. doi: 10.1007/978-3-031-01942-5_51.

[23] G. Falekas, A. Karlis, Digital Twin in Electrical Machine Control and Predictive Maintenance: State-of-the-Art and Future Prospects, Energies 14 (18) (Jan. 2021) 5933.

[24] V. Rjabtšikov *et al.*, "Digital Twin Service Unit for AC Motor Stator Inter-Turn Short Circuit Fault Detection," in *2021 28th International Workshop on Electric Drives: Improving Reliability of Electric Drives (IWED)*, Jan. 2021, pp. 1–5. doi: 10.1109/IWED52055.2021.9376328.

[25] S. Bouzid, P. Viarouge, J. Cros, Real-Time Digital Twin of a Wound Rotor Induction Machine Based on Finite Element Method, Energies 13 (20) (Jan. 2020) 5413.

[26] V. Mukherjee, T. Martinovski, A. Szucs, J. Westerlund, and A. Belahcen, "Improved Analytical Model of Induction Machine for Digital Twin Application," in *2020 International Conference on Electrical Machines (ICEM)*, Aug. 2020, pp. 183–189. doi: 10.1109/ICEM49940.2020.9270916.

[27] B. Lu, T.G. Habetler, R.G. Harley, A survey of efficiency-estimation methods for in-service induction motors, IEEE Trans. Ind. Appl. 42 (4) (Jul. 2006) 924–933, https://doi.org/10.1109/TIA.2006.876065.

[28] E. Szychta, L. Szychta, Collective Losses of Low Power Cage Induction Motors—A New Approach, Energies 14 (6) (Jan. 2021) 1749.

[29] S. Xue, J. Feng, S. Guo, J. Peng, W.Q. Chu, Z.Q. Zhu, A New Iron Loss Model for Temperature Dependencies of Hysteresis and Eddy Current Losses in Electrical Machines, IEEE Trans. Magn. 54 (1) (Jan. 2018) 1–10, https://doi.org/10.1109/TMAG.2017.2755593.

[30] H. Zhang, P. Zanchetta, K.J. Bradley, C. Gerada, A Low-Intrusion Load and Efficiency Evaluation Method for In-Service Motors Using Vibration Tests With an Accelerometer, IEEE Trans. Ind. Appl. 46 (4) (Jul. 2010) 1341–1349, https://doi.org/10.1109/TIA.2010.2049550.

[31] A.G. Siraki, C. Gajjar, M.A. Khan, P. Barendse, P. Pillay, An Algorithm for Nonintrusive In Situ Efficiency Estimation of Induction Machines Operating With Unbalanced Supply Conditions, IEEE Trans. on Ind. Applicat. 48 (6) (Nov. 2012) 1890–1900, https://doi.org/10.1109/TIA.2012.2225813.

[32] M. Al-Badri, P. Pillay, P. Angers, A Novel In Situ Efficiency Estimation Algorithm for Three-Phase Induction Motors Operating With Distorted Unbalanced Voltages, IEEE Trans. on Ind. Applicat. 53 (6) (Nov. 2017) 5338–5347, https://doi.org/10.1109/TIA.2017.2728786.

[33] S. Aheleroff, X. Xu, R.Y. Zhong, Y. Lu, Digital Twin as a Service (DTaaS) in Industry 4.0: An Architecture Reference Model, Adv. Eng. Inf. 47 (Jan. 2021), https://doi.org/10.1016/j.aei.2020.101225 101225.

[34] M. Liu, S. Fang, H. Dong, C. Xu, Review of digital twin about concepts, technologies, and industrial applications, J. Manuf. Syst. 58 (Jan. 2021) 346–361, https://doi.org/10.1016/j.jmsy.2020.06.017.

[35] K. A. Hribernik, L. Rabe, J. Schumacher, and K. -d Thoben, "Centric Information Management Concept.".

[36] M.A. Pisching, M.A.O. Pessoa, F. Junqueira, D.J. dos Santos Filho, P.E. Miyagi, An architecture based on RAMI 4.0 to discover equipment to process operations required by products, Comput. Ind. Eng. 125 (Nov. 2018) 574–591, https://doi.org/10.1016/j.cie.2017.12.029.

[37] N. Firdaus, H.A. Samat, N. Mohamad, Maintenance for Energy efficiency: A Review, IOP Conf. Ser.: Mater. Sci. Eng. 530 (1) (Jun. 2019), https://doi.org/10.1088/1757-899X/530/1/012047 012047.
[38] S. M. E. Sepasgozar, "Differentiating Digital Twin from Digital Shadow: Elucidating a Paradigm Shift to Expedite a Smart, Sustainable Built Environment," *Buildings*, vol. 11, no. 4, Art. no. 4, Apr. 2021, doi: 10.3390/buildings11040151.
[39] S. Chakraborty, S. Adhikari, R. Ganguli, The role of surrogate models in the development of digital twins of dynamic systems, Appl. Math. Model. 90 (Feb. 2021) 662–681, https://doi.org/10.1016/j.apm.2020.09.037.
[40] "IEEE Std 112-2004, IEEE Standard Test Procedure for Polyphase Induction Motors and Generators," pp. 87.
[41] A. Nikbakhsh, H.R. Izadfar, M. Jazaeri, Classification and comparison of rotor temperature estimation methods of squirrel cage induction motors, Measurement 145 (Oct. 2019) 779–802, https://doi.org/10.1016/j.measurement.2019.03.072.
[42] M. S. Jiménez Molina, "Multiphysics analysis of a high loss induction motor.," 2020, Accessed: Sep. 22, 2022. [Online]. Available: http://repositorio.udec.cl/jspui/handle/11594/4681.
[43] R. Kumar and P. Kumar, "Modelling of Stray-Load Loss for Medium Power Induction Motors," in *IECON 2018 - 44th Annual Conference of the IEEE Industrial Electronics Society*, Oct. 2018, pp. 571–576. doi: 10.1109/IECON.2018.8591650.
[44] B. A. Nasir, "Modeling of stray losses in equivalent circuit of induction machines," *AIP Conference Proceedings*, vol. 2307, no. 1, p. 020006, Dec. 2020, doi: 10.1063/5.0032902.
[45] J.-S.-R. Jang, ANFIS: adaptive-network-based fuzzy inference system, IEEE Trans. Syst. Man Cybern. 23 (3) (May 1993) 665–685, https://doi.org/10.1109/21.256541.
[46] O.M. Olatunji, I.T. Horsfall, E. Ukoha-Onuoha, K. Osa-aria, Application of hybrid ANFIS-based non-linear regression modeling to predict the %oil yield from grape peels: Effect of process parameters and FIS generation techniques, Cleaner Eng. Technol. 6 (Feb. 2022), https://doi.org/10.1016/j.clet.2021.100371 100371.
[47] F. Corcoles, J. Pedra, M. Salichs, L. Sainz, Analysis of the induction machine parameter identification, IEEE Trans. Energy Convers. 17 (2) (Jun. 2002) 183–190, https://doi.org/10.1109/TEC.2002.1009466.
[48] A.T. de Almeida, F.J.T.E. Ferreira, G. Baoming, Beyond Induction Motors—Technology Trends to Move Up Efficiency, IEEE Trans. Ind. Appl. 50 (3) (May 2014) 2103–2114, https://doi.org/10.1109/TIA.2013.2288425.
[49] A.J. Fofanah, I. Kalokoh, K.T. Hwase, A.P. Namagonya, Adaptive Neuro-Fuzzy Inference System with Non-Linear Regression Model for Online Learning Framework, IJSER 11 (8) (Aug. 2020), https://doi.org/10.14299/ijser.2020.08.01.
[50] J. K. E. da C. Martins, F. M. U. de Araújo, "Nonlinear System Identification based on Modified ANFIS," presented at the 12th International Conference on Informatics in Control, Automation and Robotics, Dec. 2022, pp. 588–595. Accessed: Dec. 28, 2022. [Online]. Available: https://www.scitepress.org/Link.aspx?doi=10.5220/0005544905880595.
[51] K.V. Singh, H.O. Bansal, D. Singh, Hardware-in-the-loop Implementation of ANFIS based Adaptive SoC Estimation of Lithium-ion Battery for Hybrid Vehicle Applications, J. Storage Mater. 27 (Feb. 2020), https://doi.org/10.1016/j.est.2019.101124 101124.